Automatica, Vol. 29, No. 6, pp. 1395–1410, 1993
Printed in Great Britain.

0005–1098/93 $6.00 + 0.00

Robust Performance of Cross-directional Basis-weight Control in Paper Machines*†

DANIEL L. LAUGHLIN,‡§ M. MORARI‡|| and RICHARD D. BRAATZ‡¶

A method is developed to design decentralized cross-directional controllers for paper machines which possess robust stability, robust performance and failure tolerance properties.

Key Words—Basis-weight; cross-directional control; decentralized control; failure tolerance; moisture content; paper industry; paper machine; pulp industry; robust control.

Abstract—The cross-machine-direction (CD) control problem in paper machines is analysed from the viewpoint of *robust performance*. The objective of robust performance is to maintain control system stability and to satisfy a bound on the maximum singular value of the closed-loop sensitivity function despite modelling error. Characteristics common to all CD response control problems including paper basis-weight control are identified. The response of an important actuator for basis-weight control, the paper machine slice, is described by a single dimensionless design parameter that provides considerable insight about the CD response control problem. Sufficient conditions allowing design of robust diagonal controllers are developed. Robust stability, performance and failure tolerance properties of the controllers are proven.

1. INTRODUCTION

THE CROSS-MACHINE-DIRECTION (CD) control problem in paper machines is aimed at maintenance of flat profiles of paper sheet properties across the paper machine. Basis-weight, or paper weight per unit area, is an example of one important sheet property. Variations in CD basis-weight can result in paper that will not lie flat. Successful control of CD paper sheet properties can mean significant reductions in raw material consumption. For example, Eastman Kodak reported a 2·4% reduction in fiber usage as a result of CD control (Carey *et al.*, 1975). Minimal variation in CD sheet properties enables operators to produce thinner paper closer to the target caliper. Additional motivations cited for better CD control in the paper manufacturing industry include: increasing demand for greater production rates; improving product quality despite a high turnover rate in the work force resulting in inexperienced operators; eliminating breaks, rewinds and rejects; and reducing energy consumption (Wallace, 1981).

1.1. *Control system robustness objective*

The purpose of this paper is to analyse the CD response control problem from the perspective of *robust performance*. In this section the objective of robust performance is mathematically defined. The formulation is done in a manner consistent with the theory of Doyle (1982, 1987). First, a set of possible models Π is used to express uncertainty in knowledge of the physical system to be controlled. Control system requirements are then proposed—two universal requirements for the control system illustrated in Fig. 1 are stability and acceptable attenuation of the disturbance in the output. If a controller satisfies these requirements for the whole set Π, it is said to exhibit robustness with respect to the modelling errors. Exactly what is meant by stability and acceptable attenuation of disturbances is defined in the following two sections.

1.1.1. *Robust stability*. Nominal stability of the control system in Fig. 1 for one process model $\tilde{P}(s) \in \Pi$ and robust stability for the whole set Π are defined as follows.

Definition 1. Nominal stability: the control system in Fig. 1 with controller $C(s)$ and process

* Received 19 July 1989; revised 3 February 1992; revised 28 January 1993; received in final form 24 February 1993. The original version of this paper was not presented at any IFAC meeting. This paper was recommended for publication in revised form by Associate Editor B. W. Bequette under the direction of Editor H. Austin Spang III.

† A short version of this paper was presented at the 1989 American Control Conference.

‡ Chemical Engineering 210-41, California Institute of Technology, Pasadena, CA 91125, U.S.A.

Author to whom correspondence should be addressed. Tel. (818) 395-4186; Fax (818) 568-8743; E-mail mm@imc.caltech.edu.

§ Current address: General Mills, Inc., 9000 Plymouth Ave., North, Minneapolis, MN 55427, U.S.A.

|| Current address: DuPont Experimental Station, P.O. Box 8010, Wilmington, DE 19880, U.S.A.

¶ Supported by the John and Fannie Hertz Foundation.

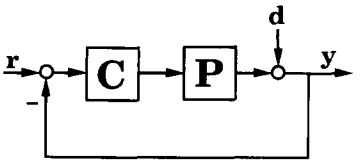

FIG. 1. Standard feedback control system with process $P(s)$, controller $C(s)$, set point $r(s)$, disturbances $d(s)$ and output $y(s)$.

$\tilde{P}(s)$ is stable if and only if all of its closed-loop poles are in the left half plane.

Definition 2. Robust stability: the control system in Fig. 1 with controller $C(s)$ and process $P(s) \in \Pi$ is robustly stable if and only if it is stable for all $P(s) \in \Pi$.

1.1.2. *Robust performance.* Before defining robust performance, it is necessary to define what is meant by *performance* of the control system in Fig. 1. The performance is defined in terms of a weight $W(s)$ restricting the magnitude (maximum singular value) of the closed-loop sensitivity function $[I + P(s)C(s)]^{-1}$.

Definition 3. Nominal performance: the control system in Fig. 1 with controller $C(s)$ and process $P(s) = \tilde{P}(s)$ exhibits nominal performance if and only if it is nominally stable and

$$\sup_{s=i\omega} \sigma_{\max}(W(s)[I + P(s)C(s)]^{-1}) < 1. \quad (1)$$

Since the sensitivity function relates system outputs $y(s)$ to disturbances $d(s)$ it is desirable that it have low magnitude. It is convenient to select a weight $W(s)$ equal to a scalar weight $w(s)$ times identity, with $w(s)$ given by

$$w(s) = b\frac{as + 1}{as} \quad (2)$$

with parameter $0 < b < 1$ and parameter $a > 0$. If a control system satisfies the performance requirement (1) with weight $w(s)$ given by (2), it will have a bandwidth of at least $1/a$ and the maximum disturbance amplification will be less than $1/b$. The concept of robust performance now follows from that of nominal performance.

Definition 4. Robust performance: the control system in Fig. 1 with controller $C(s)$ and process $P(s) \in \Pi$ exhibits robust performance if and only if it is nominally stable and the bound (1) is satisfied for all $P(s) \in \Pi$.

Define

$$\mu(\omega) \equiv \sup_{P(i\omega)\in\Pi} \sigma_{\max}(w(i\omega)(I + P(i\omega)C(i\omega))^{-1});$$

then we have from Definition 4 that robust performance is satisfied if and only if the system is nominally stable and $\mu(\omega) < 1$ for all ω. The relationship between $\mu(\omega)$ and Doyle's structured singular value (SSV) for weighted sensitivity problems is well-known (for example, see Theorem 5.4 in Packard, 1988). We use $\mu(\omega)$ instead of the SSV because $\mu(\omega)$ is a direct measure of the performance of the system for the specified set of plants. The results of this paper do not depend on which measure of performance is used.

1.2. *Controller design strategy*

Design procedures are presented in Section 6 that result in diagonal and model-inverse-based controllers for CD response control systems with typically large dimensions (large numbers of inputs and outputs). In Sections 4 and 5 it is shown that the eigenvalues of useful CD response models can be bounded on a segment of the positive real axis. The segment is then interpreted as gain uncertainty in a SISO process model of the form $p(s)$ given in (3).

$$\pi = \left\{ p(s) \mid p(s) = k\left[\frac{a_q n_q(s) + \cdots + a_1 n_1(s) + a_0 n_0(s)}{b_r d_r(s) + \cdots + b_1 d_1(s) + b_0 d_0(s)}\right] e^{-\theta s} \right\}$$
$$a_i \in [a_{i_{\min}}, a_{i_{\max}}], \quad b_j \in [b_{j_{\min}}, b_{j_{\max}}], \quad (3)$$
$$\forall i \in [1, q], \quad \forall j \in [1, r]$$
$$k \in [k_{\min}, k_{\max}], \quad \theta \in [\theta_{\min}, \theta_{\max}].$$

In (3) the terms $n_j(s)$, and $d_l(s)$ are exact functions, while real numerator coefficients a_i, denominator coefficients b_j, gain k and time-delay θ are bounded by minimum and maximum values. Since the real parameters in (3) are inexactly known, π in (3) represents a set of process models. Laughlin *et al.* (1986) show how to design a robust SISO controller $c(s)$ via internal model control for processes given by the uncertainty description in (3). This paper shows how to design robust MIMO CD response control systems from the SISO controller.

Analysis tests used to ensure that SISO controllers $c(s)$ exhibit robust performance are based on regions $\pi(i\omega)$ on the complex plane containing all possible $p(i\omega)$ in (3). A method for locating these regions can be found in Laughlin *et al.* (1986). Once these regions are located, a convenient test for SISO robust stability based on the familiar Nyquist stability test can be applied.

2. MODEL DEVELOPMENT FOR CROSS-DIRECTIONAL RESPONSE

Models relating the response of CD paper sheet properties to actuator adjustments are

required before control strategies can be developed for the paper machine. One distinctive characteristic of all such models is that they are of large dimension. Beecher and Bareiss (1970) report a 6.096-m-wide machine with 40 actuators spaced 15.24 cm apart across the slice. Up to 50 slice actuators are reported by Karlsson *et al.* (1982). Paper machines requiring response models as large as 100×100 are referenced in the literature (Wilhelm and Fjeld, 1983). Moreover, an established trend is for new machines to become wider and faster, increasing the dimension of the system and making control more difficult (Wallace, 1981).

In practice the true CD profile on paper machines is not measured—the profile at discrete points along the cross-direction is estimated from measurements obtained from a scanning gauge which continuously travels back and forth across the paper (how to perform this estimation is discussed in Bergh and MacGregor, 1987). It is these CD profile estimates that are made available to the CD controller (any additional error due to the estimation can easily be included in the uncertainty description). We assume that the number of CD profile estimates is equal to the number of actuators. We also assume that the response of CD paper sheet properties to actuator adjustments is stable; that is, the CD sheet profile settles following actuator adjustment to a point where successive measurements are nearly identical. These are reasonable assumptions for most paper machines.

2.1. *Actuator dynamics, time-delay, and interactions*

Features common to all CD response models are actuator dynamics, time-delay and interactions. A paper machine slice is designed so that it can be adjusted upward or downward by actuators at evenly spaced points along its length. No matter what mechanism is used to manipulate the slice, it is commonly assumed that every actuator along the slice can be modelled by the same dynamics (Wilhelm and Fjeld, 1983). This means that scalar actuator dynamics (for example a first-order lag $p_a(s) = k_a/(\tau_a s + 1)$) multiplies the entire matrix transfer function used to model CD response. Since basis-weight, moisture or caliper measurements are taken some distance down the machine-direction from the slice, time passing before actuator manipulations are sensed must be included in the CD response model as delay $p_d(s) = e^{-\theta s}$. The importance of this delay in CD response models varies from machine to machine as production speeds vary from less than 1 m sec^{-1} of paper to over 10 m sec^{-1}.

When one actuator is manipulated, CD sheet properties invariably change from some distance either side of the position directly downstream from the actuator. These observed interactions are incorporated into the CD response model for n actuators through a constant matrix $P_{CD}^{n,m}$. It is usually assumed that interactions are the same for all actuator locations across the paper machine. Moreover, interactions are assumed to be symmetric about each actuator location. These assumptions cause matrix $P_{CD}^{n,m}$ to take on a "banded symmetric" structure as indicated in (4). Matrix $P_{CD}^{n,m}$ can therefore be identified by measuring the CD sheet response to changes made at a single actuator—saving huge experimental effort when the slice has as many as 100 actuators.

$$P_{CD}^{n,m} = \underbrace{\begin{pmatrix} p_1 & p_2 & \cdots & p_m & 0 & \cdots & \cdots & 0 \\ p_2 & p_1 & p_2 & \cdots & p_m & \ddots & \ddots & \vdots \\ \vdots & p_2 & p_1 & p_2 & \cdots & \ddots & \ddots & \vdots \\ p_m & \vdots & p_2 & \ddots & \ddots & \vdots & p_m & 0 \\ 0 & p_m & \vdots & \ddots & \ddots & p_2 & \vdots & p_m \\ \vdots & \ddots & \ddots & \cdots & p_2 & p_1 & p_2 & \vdots \\ \vdots & \ddots & \ddots & p_m & \cdots & p_2 & p_1 & p_2 \\ 0 & \cdots & \cdots & 0 & p_m & \cdots & p_2 & p_1 \end{pmatrix}}_{n \times n} \tag{4}$$

Occasionally, elements in $P_{CD}^{n,m}$ near the upper left and lower right corners are modified to represent slight differences in CD response near the edges of the paper machine. The overall dynamic model for CD response $P_{CD}^{n,m}(s)$ is given by the product of $p_a(s)$, $p_d(s)$ and $P_{CD}^{n,m}$.

2.2. *Model parameter uncertainties*

Model uncertainty is inevitable in CD response. During normal operation, a paper machine experiences changes in speed, vacuum and other wet end process conditions that affect CD response in both magnitude and shape (Richards, 1982). Headbox hydraulics are complicated and are subject to change with changing pulpwood characteristics. Time-delay can vary significantly: Beecher and Bareiss (1970) report production speeds from 0.762 to 3.81 m sec^{-1} on a single paper machine. There are two ways to handle variations in time-delay: (1) apply gain-scheduling on the time-delay, or (2) design a single controller by treating the time-delay as being uncertain, but in some known range. If the second method were used, the paper machine above would have 67%

uncertainty in the time-delay θ. These and other uncertainties in the physical process are included in the set of process models $\Pi_{CD}^{n,m}$ defined by

$$\Pi_{CD}^{n,m} = \left\{ P_{CD}^{n,m}(s) \;\middle|\; \begin{matrix} P_{CD}^{n,m}(s) = p(s)P_{CD}^{n,m} \\ p(s) \in \pi \end{matrix} \right\} \quad (5)$$

where real elements p_i in the interaction matrix $P_{CD}^{n,m}$ are bounded as in

$$p_i \in [p_{i_{min}}, p_{i_{max}}]$$

and the set π is given by (3). For example, consider first-order actuator dynamics with time-delay:

$$\pi = \left\{ p(s) \mid p(s) = p_a(s)p_d(s) = \frac{k_a e^{-\theta s}}{\tau_a s + 1} \right\}$$
$$k_a \in [k_{a_{min}}, k_{a_{max}}], \quad \tau_a \in [\tau_{a_{min}}, \tau_{a_{max}}], \quad (6)$$
$$\theta \in [\theta_{min}, \theta_{max}].$$

Each real parameter in the scalar dynamics in (6) is allowed to vary between the specified upper and lower bounds independent of the other real parameters. Note that the other scalar dynamics in (6) are possible, though the choice of first-order with time-delay is often appropriate for the CD paper sheet response model. Uncertainity in actuator dynamics (6) is represented by the bounds for k_a and τ_a; time-delay uncertainty, by the bounds for θ.

Uncertainty in the CD interaction matrix $P_{CD}^{n,m}$ is conveniently expressed by $p_i \in [p_{i_{min}}, p_{i_{max}}]$ in model (4). This type of correlated coefficient uncertainty in $P_{CD}^{n,m}$ can naturally reflect observed deviations in experimentally measured CD response interactions. McFarlin (1983) cites ignorance of such interaction uncertainty as a probable cause of instability in CD response control systems.

2.3. *Properties of cross-directional model*

The proposed or experimental models in Table 1 of interactions in CD basis-weight response to a change at actuator p_1 are reported in the literature. They have been normalized so that response at position p_1 is 1.0. Note that the reported references have P_{CD} models of the form discussed in this paper.

The extent of interaction in CD response varies considerably among the models reported in the literature. The data from Karlsson *et al.* (1982) indicate that there is some correlation between thicker product and interactions extending over a greater number of actuator positions on the slice. Negative CD response elements can be found in many of the models reflecting the observation that efforts to increase the basis-weight downstream from one actuator position may actually decrease it on either side of that position. Strong interactions lead to large positive and negative off-diagonal elements in matrix P_{CD}^{n} in the response model. It has been reported that such strong interactions cause difficulties in the control of CD response.

On more fundamental grounds it has been shown that the system characteristics discussed below are *necessary* for the design of a CD control system to be possible which provides good performance and has other desirable fault tolerance and tuning properties.

Low condition number. A measure of the severity of expected control difficulty is the condition number γ of the CD response model,

$$\gamma(P_{CD}^{n,m}) = \frac{\sigma_{max}(P_{CD}^{n,m})}{\sigma_{min}(P_{CD}^{n,m})}. \quad (7)$$

That high condition number processes can be difficult to control is well understood—Skogestad

TABLE 1. REPORTED CD RESPONSE DOWNSTREAM FROM ACTUATOR POSITIONS

	p_1	p_2	p_3	p_4	p_5	p_6	p_7	p_8	p_9	p_{10}
(1)*	1.0	1.2	0.6	−0.4	−0.9	−0.2	−0.2			
(2)	1.0	0.4	−0.5	0.05						
(3)	1.0	0.4								
(4)	1.0	−0.15	0.03	−0.01						
(5)	1.0	0.2								
(6)	1.0	0.4								
(7)	1.0	0.5	−0.5							
(8)*	1.0	0.1	−0.3							
(9)*	1.0	1.3	0.8	−0.6	−0.3	0.0	−0.1			
(10)*	1.0	0.9	0.7	0.8	1.0	0.6	−0.5	−0.4	−0.2	−0.2
(11)*	1.0	0.45	−0.55							
(12)*	1.0	0.4	−0.2	−0.4	−0.2					
(13)*	1.0	0.2	−0.1	−0.1						

Models marked with * appear to be actual process data.

Sources: (1) "Swedish Research Labs" (Wallace, 1981); (2) (Wilkinson and Hering, 1983); (3) (Boyle, 1978); (4) actuator model (Tong, 1976); (5), (6), (7) (Wilhelm and Fjeld, 1983); (8), (9), (10) newsprint, sack paper and paper board, respectively, from Karlsson and Haglund (1983) discretized here at 20-cm actuator spacing; (11) (Richards, 1982); (12) (Cuffey, 1957); (13) change in slice opening only (Cuffey, 1957).

and Morari (1988) discuss the properties of high condition number processes at length. High condition number of the CD response model means that strong control action is required to attenuate disturbances entering the process in the direction of the left singular vector corresponding to the minimum singular value. Strong control action taken in the wrong direction, however, can lead to instability or poor performance. It is therefore difficult or impossible to design an acceptable controller based on CD response models with high condition number, when input uncertainty or uncorrelated interaction-element uncertainty is also present. Efforts must be taken to avoid these types of model uncertainty descriptions when they are not physically motivated, so that a controller with good performance can be designed.

In the limit of $\gamma \to \infty$, the CD response model $P_{CD}^{n,m}$ is singular. If this is the case, CD response is uncontrollable because upstream actuator positions causing measured downstream response profiles cannot be determined. That strong enough interactions could result in a singular CD response model was recognized by Wilhelm and Fjeld (1983). Paper machines must be constructed to have nonsingular $P_{CD}^{n,m}$ so that CD control is possible.

For CD interactions $P_{CD}^{n,m}$ as given by (4), the condition number γ is a function of both interaction and *dimension*. Figure 2 illustrates the condition number of $P_{CD}^{n,m}$ with elements $p_1 = 1.0$, $p_2 = r$, and $p_3 = -r$ for $0 \le r \le 0.5$ as a function of model dimension n. The plot has been truncated at $\gamma = 50.0$ to improve scale—γ increases to ∞ above each of the "flat" peaks in the plot. For values of r greater than 0.25, models of all dimensions $6 \le n \le 20$ have at least one singularity. Values of r at which singularities occur change dramatically as the dimension of the system changes. Given the level of interaction $r = 0.424$, for example, a 7×7 system has relatively low condition number

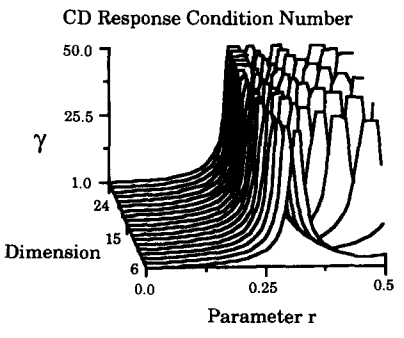

FIG. 2. Condition number of $P_{CD}^{n,3}$ with $p_1 = 1$, $p_2 = r$ and $p_3 = -r$.

$\gamma = 6.77$, while a 14×14 system is singular. Building a paper machine twice the width of one on which CD control is easily accomplished can result in CD response that is impossible to control.

Positive loop gain. Let the controller $C(s)$ in Fig. 1 be of the form $C(s) = (k/s)C'(s)$ where $C'(0)$ is bounded. Then it can be shown (Morari, 1985) that the closed-loop system will be *unstable* for arbitrarily small values of k when any of the eigenvalues of $P(0)C'(0)$ are in the left half plane. The implications for CD control are profound. Assume that a simple scalar control system is desired: $C(s) = c(s) \cdot I$, where $c(s)$ is a scalar controller with integral term. Such a design is feasible in practice only if all eigenvalues of the CD response model $P_{CD}^{n,m}$ are restricted to a half plane or in the case of a symmetric $P_{CD}^{n,m}$, if $P_{CD}^{n,m}$ is positive definite.

Assume on the other hand that the control system is of the steady-state-inverse type as has been reported in the literature. Then $P(0)C'(0) = I$ and no problems arise. If $P(0)$ is ill-conditioned, however, then even for small errors in the model of $P(0)$ [the design basis for $C'(0)$], $P(0)C'(0) \neq I$ and some of the eigenvalues of the product can very well fall into the left half plane. Then the closed-loop system will be *unstable*, even if the actuators are adjusted infrequently in pseudo-steady-state fashion.

Fault tolerance. Often it is desirable to design a set of SISO controllers so that the overall system remains stable even when some actuators are taken out of service. It can be shown (Morari and Zafiriou, 1989) that for this to be possible it is again necessary that all eigenvalues of $P_{CD}^{n,m}$ be in the right half plane.

In summary, for good control it is essential that the actuator be designed such that the CD response model is well conditioned. For good failure tolerance and to allow simple control structures it is also desirable that P_{CD} be positive definite. These characteristics are analyzed later in the paper for the models in Table 1.

2.4. *Slice actuator design to influence interactions*

The design of the paper machine slice has a significant effect on the interactions in CD response. The actuators must be located near enough to one another so that narrow uneven streaks in the paper can be eliminated. However, each actuator–slice junction can behave as a fulcrum, causing negative elements in the CD response model (Cuffey, 1957). Wilhelm states that strong interaction in the CD response model is the result of poor choice of actuator spacing (Wilhelm and Fjeld, 1983). Interactions introduced at the slice propagate

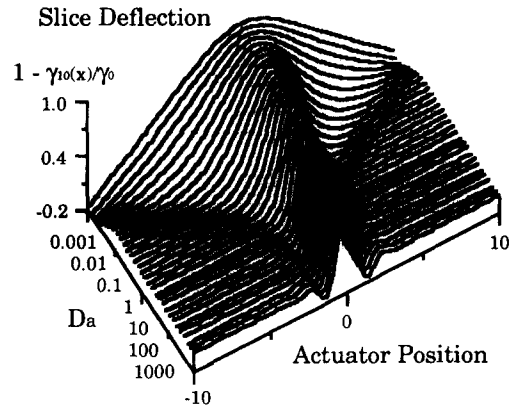

FIG. 3. Deflection of the slice actuator as a function of the dimensionless design parameter D_a.

down the paper machine and can often be exacerbated by subsequent processing steps. The nature of interactions introduced and the balance between design parameters have been investigated by Laughlin (1988) who modelled the slice as a beam supported by springs equally spaced at actuator locations. It was found that the displacement of the slice at the actuator positions depends on the dimensionless slice actuator design parameter $D_a = k_s a^3/6EM$ which is related to the Winkler spring constant. Here k_s is the spring constant, a is the distance between actuators, E is the elastic modulus of the beam, and M is the moment of inertia of the beam cross-section. The limiting behavior of slice displacement for extreme values of D_a is easy to interpret physically and mathematically. For $D_a = 0$ the slice is perfectly rigid and level; for $D_a = \infty$ the springs representing the actuators are perfectly rigid causing the slice to bend between their fixed endpoints. This behavior and other slice displacements for intermediate values of D_a are illustrated in Fig. 3. Note that deflection of the slice is negative for certain actuator positions on either side of center—this accounts for negative elements in the CD response model.

Tong proposed that the slice be modelled as a beam in simple bending between rigid actuators—such a model corresponds to the limit $D_a \to \infty$. Interactions labeled 4 in Table 1 were calculated from his model (Tong, 1976). The extension of such a model to allow for compressible actuators provides insight about how the slice might be designed to suppress interactions.

The effect of slice design on condition number and therefore on achievable control quality will be illustrated later in the paper.

2.5. *Wave propagation on the Fourdrinier*

Slice deflection alone cannot account for the magnitude of some of the larger negative off-diagonal elements in CD response models in Table 1. Bernoulli's equation applied to flow under the slice results in velocity proportional to the slice opening. If no further effects are taken into account, CD response models with small negative off-diagonal elements like (4) from Tong (1976) result. Water waves on the Fourdrinier wire can propagate interactions introduced by the slice even further along the cross-machine-direction. Wrist (1961) reports a study showing that radioactively marked fibers traveled 15.24 cm in the cross-machine-direction through the wet end of a newsprint machine producing paper at a rate 8.128 m sec^{-1}. Behavior of the water waves is similar to that of a wake behind a ship—waves propagate in a "V" formation downstream from the location where an actuator is adjusted. An analysis by White (1979) indicates that higher waves will travel faster in the cross-machine-direction on the Fourdrinier wire than will lower waves. The effect of this is to flatten the peak of the wave exiting at the center of the slice opening in Fig. 3. Since interactions in CD response elements are normalized so that the center response is one, the off-diagonal elements become proportionately larger. The magnitude of this effect is, of course, dependent on machine speed, product caliper, fluid properties of the furnish fiber suspension, speed of deposition of fibers on the Fourdrinier wire, length of the wire, mechanical shake applied to the wire etc.

3. REPORTED CONTROL STRATEGIES

Control systems for regulation of CD paper sheet properties have been on line in paper mills for some time (e.g. see Beecher and Bareiss, 1970; or Carey *et al.* 1975). Two control schemes are reported in the literature for CD response control in paper manufacturing: linear-quadratic-optimal (LQ) and model-inverse-based control. The following researchers report using LQ controller design methods minimizing quadratic cost functions penalizing both deviations in paper sheet properties and slice position: Wilhelm and Fjeld (1983), Tong (1976), Boyle (1978), Richards (1982) and Wilkinson and Hering (1983). Mostly steady-state models are proposed—interaction matrices $P_{CD}^{n,m}$. New control actions are often taken only after steady state is reached. In model-inverse-based controllers the inverse of $P_{CD}^{n,m}$ is used to define control actions (Wilkinson, 1983). Often $P_{CD}^{n,m}$ is identified on-line and used in some type of adaptive control scheme. Additional review of control methods applied to the paper manufac-

turing industry can be found in the article by Dumont (1986).

One weakness of reported controller design techniques is that they do not address the issue of robustness with respect to errors in the CD response model. In light of the many difficult-to-model process characteristics, for example, wave propagation on the Fourdrinier wire, such modelling errors are inevitable. A more satisfactory controller design technique would guarantee system stability and performance despite modelling errors. Another weakness of both model-inverse-based controller design methods and LQ controller design methods is that they lead to complicated control algorithms for large dimension systems. The inverse of a band diagonal CD interaction model $P_{CD}^{n,m}$ is in general a full matrix—a 100×100 system would lead to a controller with 10,000 elements. A more desirable controller structure would be diagonal or band-diagonal so that paper sheet properties at one point could be controlled by manipulating a few actuators on either side. Later in this paper, a robust controller design procedure is developed that results in a diagonal controller structure. A robust controller design procedure that results in banded controllers is developed in Laughlin (1988).

4. SPECIAL MODELS FOR CROSS-DIRECTIONAL SHEET PROPERTIES

Special properties of three models for CD response enable convenient robust controller design despite correlated parameter uncertainties in response interactions. The models are centrosymmetric, Toeplitz symmetric and circulant symmetric matrices. General examples and selected properties of the three special CD interaction matrices are given in this section. Nomenclature for these matrix forms is standard in the mathematics literature—additional properties of the three forms can be found in the works by Davis (1979), Bellman (1970) and Aitken (1954). Transformations relating the three forms are presented that allow development of tight bounds on CD response model eigenvalues despite parameter uncertainties. The bounds establish that with similar interactions the three forms closely resemble one another for large-dimension systems. This result enables development of convenient robust controller design techniques.

4.1. *Model structures*

The three special model structures, centrosymmetric, Toeplitz symmetric and circulant symmetric, imply certain assumptions about the nature of CD response interactions. Assumptions that accompany each form are given in the following three sections of this paper. It is important to consider the appropriateness of these assumptions for a particular CD control problem. Whether or not the assumptions are accurate can mean success or failure of the control system design based on one of the models.

4.1.1. *Centrosymmetric.* Centrosymmetric models have elements that are symmetric about the center of the matrix. If a paper machine were constructed to be symmetric with respect to a vertical plane through the center of the sheet, then the physical CD response would be *exactly* centrosymmetric. Centrosymmetric models can represent edge effects observed in the CD response, that is, slight differences in response observed at different distances from the center of the sheet. An example of a centrosymmetric matrix $P_{CD}^{n,m}$ is given by (8). If it is further assumed that the effect of actuator adjustment at position i on response at position j is the same as that at position j on response at position i, then

$$P_{CS}^{n,m} = \underbrace{\begin{pmatrix} p_{11} & p_{12} & \cdots & p_{1m} & 0 & \cdots & \cdots & \cdots & \cdots & 0 \\ p_{21} & p_{22} & p_{23} & \cdots & p_{2m} & 0 & \ddots & \ddots & \ddots & \vdots \\ \vdots & p_{32} & \ddots & \ddots & \cdots & \ddots & \ddots & \ddots & \ddots & \vdots \\ p_{m1} & \vdots & \ddots & p_{mm} & \ddots & \cdots & \ddots & \ddots & \ddots & \vdots \\ 0 & p_{m2} & \vdots & \ddots & \ddots & \ddots & \vdots & \ddots & 0 & \vdots \\ \vdots & 0 & \ddots & \vdots & \ddots & \ddots & \ddots & \vdots & p_{m2} & 0 \\ \vdots & \ddots & \ddots & \ddots & \cdots & \ddots & p_{mm} & \ddots & \vdots & p_{m1} \\ \vdots & \ddots & \ddots & \ddots & \ddots & \cdots & \ddots & \ddots & p_{32} & \vdots \\ \vdots & \ddots & \ddots & \ddots & 0 & p_{2m} & \cdots & p_{23} & p_{22} & p_{21} \\ 0 & \cdots & \cdots & \cdots & \cdots & 0 & p_{1m} & \cdots & p_{12} & p_{11} \end{pmatrix}}_{n \times n}. \tag{8}$$

$$P_C^{n,m} = \underbrace{\begin{pmatrix} p_1 & p_2 & \cdots & p_m & 0 & \cdots & 0 & p_m & \cdots & p_2 \\ p_2 & p_1 & p_2 & \cdots & p_m & 0 & \cdots & \ddots & \ddots & \vdots \\ \vdots & p_2 & p_1 & p_2 & \cdots & p_m & \ddots & \ddots & \ddots & p_m \\ p_m & \vdots & p_2 & p_1 & p_2 & \cdots & \ddots & \ddots & \vdots & 0 \\ 0 & p_m & \vdots & p_2 & \ddots & \ddots & \vdots & p_m & 0 & \vdots \\ \vdots & 0 & p_m & \vdots & \ddots & \ddots & p_2 & \vdots & p_m & 0 \\ 0 & \vdots & \ddots & \ddots & \cdots & p_2 & p_1 & p_2 & \vdots & p_m \\ p_m & \ddots & \ddots & \ddots & p_m & \cdots & p_2 & p_1 & p_2 & \vdots \\ \vdots & \ddots & \ddots & \cdots & 0 & p_m & \cdots & p_2 & p_1 & p_2 \\ p_2 & \cdots & p_m & 0 & \cdots & 0 & p_m & \cdots & p_2 & p_1 \end{pmatrix}}_{n \times n} \tag{9}$$

$P_{CS}^{n,m}$ is centrosymmetric *symmetric*. When $P_{CS}^{n,m}$ is symmetric it is denoted by $P_{CSS}^{n,m}$ in this paper.

4.1.2. *Toeplitz symmetric.* In Toeplitz symmetric models the same element is repeated along each diagonal of the matrix. The assumption, that changes observed downstream from one actuator caused by adjustments at the nearest neighboring actuators is independent of position across the machine, leads to a Toeplitz symmetric model. The CD response model $P_{CD}^{n,m}$ in (4) is Toeplitz symmetric—this is the CD response model most often found in the literature. Toeplitz symmetric CD response models are denoted by $P_{CD}^{n,m} = P_T^{n,m}$ in this paper.

4.1.3. *Circulant symmetric.* A circulant symmetric structure $P_C^{n,m}$ is given by (9).

For simplicity, $P_C^{n,m}$ is often written $\text{circ}(p_1, p_2, \ldots, p_m, 0, \ldots, 0, p_m, \ldots, p_2)$. Circulant symmetric matrices are both Toeplitz symmetric and centrosymmetric. As such, $P_C^{n,m}$ represents CD response interactions of a paper machine *without* edge effects similar to the truncated infinite dimensional model cited by Wilhelm and Fjeld (1983). Such a model structure is appropriate for circular machines, as are used in some plastic extrusion applications (Martino, 1991). Circulant matrices commute with one another—the eigenvalues of the product of two circulant matrices are equal to the product of the eigenvalues of the two matrices. Circulant matrices lend valuable insight about properties of related CD response models, because their eigenvalues and eigenvectors can be determined by inspection. Eigenvalues λ_i of circulant symmetric matrices are given by (10).

$$\begin{aligned} \lambda_i(\text{circ}(p_1, p_2, \ldots, p_m, 0, \ldots, 0, p_m, \ldots, p_2)) \\ = p_1 + 2\,\text{Re}\,[w_i]p_2 + 2\,\text{Re}\,[w_i^2]p_3 \\ + \cdots + 2\,\text{Re}\,[w_i^{m-1}]p_m \end{aligned} \tag{10}$$

where w_i is one of the n roots of $w^n = 1$ (for proof see Bellman, 1970). Equation (10) is a powerful tool for bounding the eigenvalues of $P_C^{n,m}$ despite correlated element uncertainties given by $p_i \in [p_{i_{\min}}, p_{i_{\max}}]$. Evaluating (10) is straightforward even when *uncertain* p_i are bounded on the real axis—addition of *uncorrelated* line segments is all that is required.

4.2. *Transformations relating special models*

Transformations given in this section relate the special models $P_{CSS}^{n,m}$ and $P_T^{n,m}$ to a *larger* circulant symmetric model $P_C^{n+2(m-1),m}$. The transformations and subsequent eigenvalue bounds will demonstrate that the three models closely approximate one another for large dimensions n—the large system dimensions usually encountered in CD paper response control. These transformations are used to prove the theorems in the following section.

Transformation 1. *Circulant symmetric to Toeplitz symmetric.* The transformation from the circulant symmetric matrix $P_C^{n+2(m-1),m}$ to the Toeplitz symmetric matrix $P_T^{n,m}$ is given by

$$P_T^{n,m} = (R_{C\to T}^{n,m})^T P_C^{n+2(m-1),m} R_{C\to T}^{n,m} \tag{11}$$

where

$$\begin{aligned} (R_{C\to T}^{n,m})^T = (0^{n\times(m-1)} \quad I^{n\times n} \quad 0^{n\times(m-1)}) \\ \in \mathcal{R}^{n\times n+2(m-1)}. \end{aligned}$$

This transformation extracts the center section of a circulant symmetric matrix, which is Toeplitz symmetric.

Transformation 2. *Toeplitz symmetric to centrosymmetric symmetric.* The transformation from the Toeplitz symmetric $P_T^{n,m}$ defined in Transformation 1 above to the centrosymmetric *symmetric* matrix $P_{CSS}^{n,m}$ is given by

$$P_{CSS}^{n,m} = (S_{CSS}^{n,m})^{1/2} P_T^{n,m} (S_{CSS}^{n,m})^{1/2} \tag{12}$$

where

$$\begin{aligned} S_{CSS}^{n,m} = \text{diag}\,(s_1, s_2, \ldots, s_x, \ldots, s_2, s_1) \\ \in \mathcal{R}^{n\times n}, \quad s_i > 0 \end{aligned}$$

is a diagonal centrosymmetric matrix with $x = n/2$ for even n or $x = (n+1)/2$ for odd n. (Scalar s_x appears twice for even n.)

5. ROBUST STABILITY AND PERFORMANCE RESULTS

The robust stability and performance results are based on the following arguments: the minimum and maximum singular values of a Toeplitz symmetric and a centrosymmetric symmetric matrix are bounded by those of a circulant symmetric matrix of larger size. Bounds on the singular values of a circulant symmetric matrix in the presence of parameter uncertainty can be easily established through (10). The proofs of the results are in the appendix.

Theorem 1. If the SISO control system with loop transfer function $kp(s)c(s)$ is robustly stable for all $p(s) \in \pi$ and all $k \in [\sigma_{\min}(P_C^{q+2(m-1),m}), \sigma_{\max}(P_C^{q+2(m-1),m})]$, where $P_C^{q+2(m-1),m}$ is positive definite symmetric, then the MIMO control systems with the loop transfer functions

$$[P_C^{n,m}p(s)]\{c(s)\}$$

$$[P_T^{n,m}p(s)]\{c(s)\}$$

$$[P_{CSS}^{n,m}p(s)]\{c(s)(S_{CSS}^{n,m})^{-1}\}$$

are robustly stable for all $p(s) \in \pi$ for all dimensions $n \le q$.

Theorem 2. If the SISO control system with loop transfer function $kp(s)c(s)$ exhibits robust performance in the sense that

$$|w(i\omega)(1 + kp(i\omega)c(i\omega))^{-1}| < 1$$

for all ω, for all $p(s) \in \pi$, and for all

$$k \in [\sigma_{\min}(P_C^{q+2(m-1),m}), \quad \sigma_{\max}(P_C^{q+2(m-1),m})],$$

where $P_C^{q+2(m-1),m}$ is positive definite symmetric, then the MIMO control systems with the loop transfer functions given in Theorem 1 exhibit robust performance for all dimensions $n \le q$ in the sense that

$$\sigma_{\max}[w(i\omega)(I + P_C^{n,m}p(i\omega)c(i\omega))^{-1}] < 1 \quad \forall\omega$$

$$\sigma_{\max}[w(i\omega)(I + P_T^{n,m}p(i\omega)(c(i\omega))^{-1}] < 1 \quad \forall\omega$$

$$\sigma_{\max}[w(i\omega)(I + P_{CSS}^{n,m}p(i\omega)c(i\omega)(S_{CSS}^{n,m})^{-1})^{-1}] < 1 \quad \forall\omega$$

for all $p(s) \in \pi$.

Not only can robust stability and robust performance of properly designed MIMO CD response control systems be guaranteed, but robust failure tolerance can be guaranteed as well. That is, *both* robust stability and robust performance requirements of the remaining system will be satisfied when one or more sensors and actuators are taken out of the control loop. Actuator/sensor failure is equivalent to premultiplication and postmultiplication of the loop transfer function by R^T and R, respectively, where $R \in \mathcal{R}^{n\times r}$ is a matrix $(r < n)$ such that $R^TR = I^{r\times r}$. Matrix R^T is such that R^TP eliminates rows of P where sensors fail. Matrix R is such that CR eliminates columns of C where actuators fail. Robust failure tolerance of MIMO CD response control systems with diagonal controllers is guaranteed when the conditions of Theorem 3 are satisfied.

Theorem 3. Let $R \in \mathcal{R}^{n\times r}$ be a matrix $(r < n)$ such that R^TA eliminates rows of A with $R^TR = I^{r\times r}$. If the SISO control system with loop transfer function $kp(s)c(s)$ exhibits robust performance in the sense that

$$|w(i\omega)(1 + kp(i\omega)c(i\omega))^{-1}| < 1$$

for all ω, for all $p(s) \in \pi$, and for all $k \in [\sigma_{\min}(P_C^{q+2(m-1),m}), \sigma_{\max}(P_C^{q+2(m-1),m})]$, where $P_C^{q+2(m-1),m}$ is positive definite symmetric, then the MIMO control systems with the loop transfer functions given in Theorem 1 premultiplied by R^T and postmultiplied by R exhibit robust failure tolerance for all dimensions $r < n \le q$ in the sense that the systems are robustly stable and

$$\sigma_{\max}[w(i\omega)(I + R^TP_C^{n,m}p(i\omega)c(i\omega)R)^{-1}] < 1 \quad \forall\omega$$

$$\sigma_{\max}[w(i\omega)(I + R^TP_T^{n,m}p(i\omega)c(i\omega)R)^{-1})] < 1 \quad \forall\omega$$

$$\sigma_{\max}[w(i\omega)(I + R^TP_{CSS}^{n,m}p(i\omega)c(i\omega)(S_{CSS}^{n,m})^{-1}R)^{-1}] < 1 \quad \forall\omega$$

for all $p(s) \in \pi$.

6. CONTROLLER SYNTHESIS METHODS

In this section two design methods utilizing results in Theorems 1–3 are presented for CD response control. The design methods lead to diagonal and full matrix transfer function controller structures. The proposed methods enable design of CD response controllers for robust performance, where previous design methods cannot be successfully applied.

Prior to this work, two alternatives existed that could theoretically address the problem of designing CD response controllers for robust performance. The first design method is DK-iteration (commonly called "μ-synthesis"), which is summarized in Doyle (1987). This method involves iterative H_∞-optimization, is only directly applicable to processes with complex uncertainties and gives high-order

full-matrix controllers. The second alternative is the robust decentralized controller design method of Skogestad and Morari (1989). It is beyond the capability of the existing software to design robust CD response controllers using either of these methods because realistic CD problem sizes involve *huge* μ problems with repeated real scalar perturbation blocks.

The following design methods *can* be easily applied to CD response control problems with many inputs and outputs. Large numbers of parameter uncertainties in the scalar dynamics and interaction parameter uncertainties can also be accommodated.

6.1. *Decentralized controller design*

It has been demonstrated that the eigenvalues of positive definite CD response interaction matrices $P_{CD}^{n,m}$ can be conveniently bounded on the real axis. By treating this segment on the real axis as uncertainty in gain k, it is possible to design a robust diagonal controller $c(s)(S^{n,m})^{-1}$ for the MIMO process $P_{CD}^{n,m}(s) = p(s)P_{CD}^{n,m}$ by designing a robust controller $c(s)$ for the SISO process $kp(s)$. The gain k can reflect CD interaction uncertainty through bounded parameters p_i in (10). Interaction uncertainty and more severe CD response interactions lead to eigenvalues on a slightly different/larger segment of the real axis. Most importantly, by treating interaction uncertainty in this way, *robust performance* of the MIMO system is implied by robust performance of the SISO system.

6.1.1. *Synthesis method.* For a CD response model with interactions given by $P_T^{n,m}$ or $P_{CSS}^{n,m}$, the diagonal controller synthesis method is outlined as follows.

(1) Determine the circulant symmetric matrix $P_C^{n+2(m-1),m}$ corresponding to the model $P_T^{n,m}$ or $P_{CSS}^{n,m}$ (these are defined in Section 4.1).
(2) Model uncertainty in SISO dynamics $p(s) = p_a(s)p_d(s)$ as in (6).
(3) Calculate $\lambda_{min}(P_C^{n+2(m-1),m})$ and $\lambda_{max}(P_C^{n+2(m-1),m})$ from (10).
(4) If $\lambda_i(P_C^{n+2(m-1),m}) > 0\ \forall i$ continue—scalar times diagonal integral control is possible only for positive definite matrices $P_C^{n+2(m-1),m}$.
(5) Select a performance weight $w(s)$ as in (2).
(6) Design a controller $c(s)$ for robust performance for the SISO process $kp(s)$ with $p(s) \in \pi$, where $k \in [\lambda_{min}(P_C^{n+2(m-1),m}), \lambda_{max}(P_C^{n+2(m-1),m})]$ (see Section 1.2).
(7) Scale MIMO controller $C(s) = c(s)I^{n\times n}$ with the appropriate matrix $(S^{n,m})^{-1}$ (from Theorem 1) for robust performance of the MIMO system. This scaling is only necessary when the plant matrix is centrosymmetric symmetric.

Alternative methods exist for the SISO robust performance problem in Step (6). The internal model control (IMC) design method presented by Laughlin *et al.* (1986) for robust performance despite model parameter uncertainties solves this problem. The IMC method involves the design of an H_2-optimal controller with a detuning filter. Increasing the filtering decreases the control action and increases robustness to model uncertainty. The control action may need to be limited to prevent damage to the slice.

6.1.2. *Example* 1. The first example problem is design of a diagonal controller for the system $P_{CD}^{20,3}(s)$ in (5), with interactions $P_{CD}^{20,3} = P_T^{20,3}$ defined as follows:

$$p_1 = 1.0; \quad p_2 \in [0.1, 0.2]; \quad p_3 \in [-0.1, -0.05]. \tag{13}$$

These values are typical of those reported in Table 1 from both experiments and theory.

Uncertain first-order actuator dynamics with time-delay are given by

$$p(s) = \frac{k_a e^{-\theta s}}{\tau_a s + 1} \tag{14}$$

$$k_a \in [0.9, 1.1]; \quad \theta \in [0.8, 1.2]; \quad \tau_a \in [0.7, 1.3].$$

Minimum and maximum eigenvalues of $P_C^{24,3}$ are given by (10) as follows:

$$\lambda_{min}(P_C^{24,3}) = 0.4$$

$$\lambda_{max}(P_C^{24,3}) = 1.3.$$

Since $P_C^{24,3}$ is positive definite, the design procedure applies. The performance weight $w(s)$ is selected to assure a bandwidth of at least 0.25 rad sec^{-1} ($b = 1/2$ and $a = 4$). Next, a SISO controller is designed for $kp(s)$ with $k \in [0.4, 1.3]$ following the IMC design procedure of Laughlin *et al.* (1986). In this case the IMC controller results in a Smith predictor controller given by

$$c(s) = \frac{1}{0.85} \frac{s+1}{2s+1-e^{-s}}. \tag{15}$$

Figure 4 is the region Nyquist plot for this example. Since none of the regions $\pi(i\omega)$ contain $(-1, 0)$, the SISO system is robustly stable. In Fig. 5, Curve 1 is $\mu(\omega)$ for this example, where $\mu(\omega)$ is the supremum of $|w(i\omega)[1 + p(i\omega)c(i\omega)]^{-1}|$ over all $p(s) \in \pi$. Since $\mu(\omega) < 1$ for all ω, sufficient conditions in Theorem 2 for robust performance of the MIMO system are satisfied.

The value of the special robustness results derived for the special structure of the CD problem can be seen from the following.

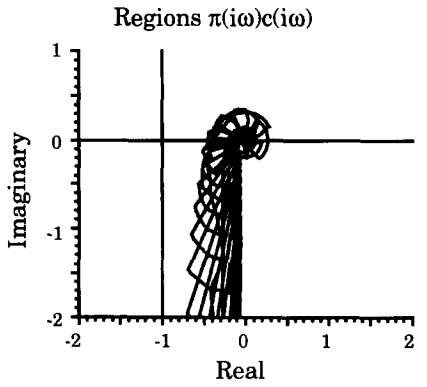

FIG. 4. Robust stability test for $kp(s)c(s)$ for all $p(s) \in \pi$ and for all $k \in [\lambda_{\min}(P_C^{24,3}), \lambda_{\max}(P_C^{24,3})]$.

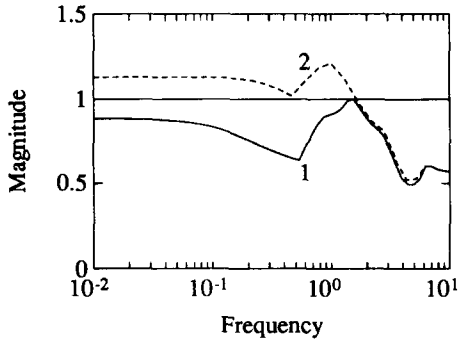

FIG. 5. Plots of $\mu(\omega)$ for the CD response control system designed in Section 6.1.2. Curve 1 is $\mu(\omega)$ for the SISO system. When $\mu(\omega)$ is less than one for all frequencies, robust performance for the MIMO system is guaranteed (by Theorem 2). Curve 2 is $\mu(\omega)$ for the MIMO system with real parameter uncertainties covered by complex uncertainties.

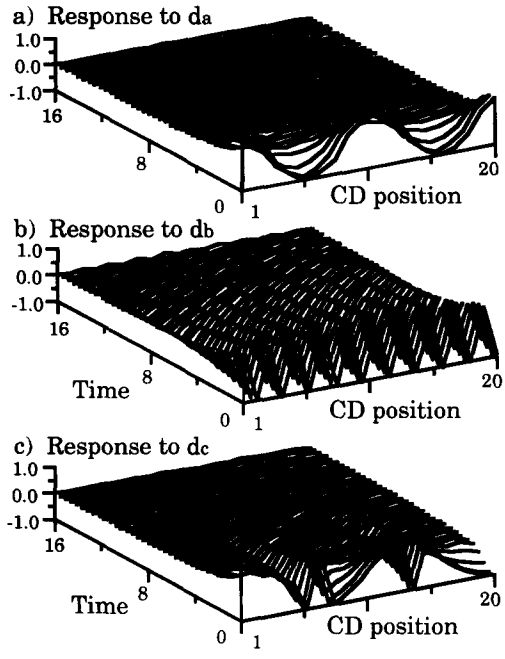

FIG. 6. Simulations of CD response to step disturbances d_a, d_b and d_c. Note that response to D_b in the direction of the vector corresponding to the minimum singular value is sluggish.

Existing structured singular value software (e.g. μ-tools, Balas *et al.*, 1991) can be used only by covering the real parameter uncertainties with complex uncertainties—this leads to the conservative estimate of $\mu(\omega)$ shown as Curve 2 in Fig. 5. The sufficient conditions from Theorem 2 for MIMO robust performance are satisfied for the 20×20 system, but existing software fails to indicate this result.

The bound for $\mu(\omega)$ from Theorem 2 is actually not conservative at all for this example. $\mu(\omega)$ for the MIMO system was calculated by extensive gridding (this took many hours on a Sun Sparcstation 2) and found to be within 1% of $\mu(\omega)$ for the SISO system (Curve 1).

The resulting MIMO controller for this example is simply $c(s)I^{20\times 20}$. Response of the closed-loop system to step disturbances is illustrated in Fig. 6. Parameters in the process model used for the simulation given by

$$p(s) = \frac{1.1e^{-0.8s}}{0.7s+1} \times \begin{pmatrix} 1.0 & 0.2 & -0.1 & 0 & \cdots & 0 \\ 0.2 & 1.0 & 0.2 & \ddots & \ddots & \vdots \\ -0.1 & 0.2 & \ddots & \ddots & \ddots & 0 \\ 0 & \ddots & \ddots & \ddots & 0.2 & -0.1 \\ \vdots & \ddots & \ddots & 0.2 & 1.0 & 0.2 \\ 0 & \cdots & 0 & -0.1 & 0.2 & 1.0 \end{pmatrix} \tag{16}$$

are far from their mean values to demonstrate controller robustness. The three step disturbances used in the simulations enter the system in different directions:

$$d_a = (1, 0.8, 0.4, -0.4, -0.8, -1, -0.8, -0.4, 0.4, 0.8, 1, 0.8, 0.4, -0.4, -0.8, -1, -0.8, -0.4, 0.4, 0.8)$$

$$d_b = (1, -1, 1, -1, 1, -1, 1, -1, 1, -1, 1, -1, 1, -1, 1, -1, 1, -1, 1, -1)$$

$$d_c = (1, 0.9, 0.7, 0.4, 0, -1, 1, -1, -0.7, -0.3, 0.3, 0.7, 1, -1, 1, 0, -0.4, -0.7, -0.9, -1).$$

Note that the response to disturbance d_b is more sluggish than that to d_a. Disturbance d_b enters with a large component in the direction of the vector corresponding to the minimum singular value and is therefore difficult to reject. This behavior could have been predicted by calculating the vector v_i corresponding to the minimum eigenvalue (and hence singular value) of the circulant symmetric matrix $P_C^{20,3} = \text{circ}(1, 0.2,$

$-0.1, 0, \ldots, 0, -0.1, 0.2)$, with $w_i = -1$ in (10). Disturbance d_a enters in a more favorable direction. The response to disturbance d_c displays elements of both favorable and unfavorable directions. We see for this example that the controller rejects disturbances with large spatial second derivatives in the cross-direction much more poorly than disturbances that have smooth spatial variation in the cross-direction. A disturbance like d_b also causes more stress on the slice—this makes a disturbance like d_b particularly bothersome. For a more detailed discussion of the effects of disturbance direction, see Skogestad *et al.* (1988).

6.2. *Model-inverse-based controller design*

In case the CD response mode is not positive definite, Laughlin (1988) discusses the design of a diagonal precompensator $C(s)$ to make it positive definite. If this scheme fails, the following technique is useful *when interaction uncertainty is small.* The SISO controller $c(s)$ is designed as in Section 6.1. The MIMO controller is calculated from $c(s)$:

$$C(s) = c(s)(\tilde{P}_{CD}^{n,m})^{-1}. \tag{17}$$

The model-inverse-based controller design procedure applied to the system with CD response model $P_{CD}^{20,3}(s)$, with exact interactions $\tilde{P}_{CD}^{20,3} = \tilde{P}_{T}^{20,3}$ defined by mean values in (13), scalar dynamics defined by (14), and performance requirement $w(s)$ defined by (2) with $b = 1/2$ and $a = 4$, leads to the controller

$$C(s) = \frac{s+1}{\epsilon s + 1 - e^{-1}}(\tilde{P}_{T}^{20,3})^{-1} \tag{18}$$

with IMC filter parameter $\epsilon = 1$. For $\epsilon = 0$, $C(s)$ is the H_2-optimal controller for step disturbances (Morari and Zafiriou, 1989). A larger ϵ detunes the H_2-optimal controller to give smaller control actions and increased robustness to model uncertainty. The control action may need to be limited to prevent damage to the slice. For simplicity, in this example we consider only the detuning required to increase robustness to model uncertainty. Detuning the controller with $\epsilon = 1$ was required to satisfy the sufficient conditions for robust performance despite parametric uncertainties in the scalar dynamics. The $\mu(\omega)$ plot for this system is illustrated as Curve 1 in Fig. 7 indicating that the robust performance objective has been met.

When CD response interaction uncertainty is significant, the above design procedure does not apply. Unless structured singular value analysis is used to evaluate robust performance with respect to interaction uncertainties and real parameter uncertainties in the scalar dynamics, the only alternative is to detune the controller for robust performance with respect to a conservative norm-bounded multiplicative uncertainty $I + L_m(s)$ with $\sigma_{max}[L_m(s)] \le |l_m(s)|$, where $|l_m(s)|$ is given by

$$|l_m(s)| = |l_i| + |l_d(s)| + |l_i|\,|l_d(s)|, \tag{19}$$

l_i is the multiplicative error representing interaction parameter uncertainties and $l_d(s)$ is the multiplicative error representing scalar dynamic uncertainties. For example, consider the uncertain interaction parameters given by (13) in model $P_{T}^{20,3}$ written in the form $P_{T}^{20,3} = \tilde{P}_{T}^{20,3}[I + (\tilde{P}_{T}^{20,3})^{-1}E_{T}^{20,3}]$, with nominal $\tilde{P}_{T}^{20,3}$ given by mean values in (13) and norm-bounded elements e_i in additive interaction error $E_{T}^{20,3}$ given by $|e_1| = 0$, $|e_2| \le 0.05$ and $|e_3| \le 0.025$. Let $E_{C}^{24,3}$ be the circulant matrix that would result in $E_{T}^{20,3}$ after "chopping off" the corners. The maximum singular value of $E_{C}^{24,3}$ is equal to 0.15 [from (10)]. Since $\sigma_{max}[E_{T}^{20,3}] \le \sigma_{max}[E_{C}^{24,3}]$ an upper bound on the magnitude of multiplicative interaction error $|l_i| = \sigma_{max}[(\tilde{P}_{T}^{n,m})^{-1}E_{T}^{20,3}]$ is easily calculated as follows:

$$|l_i| \le \sigma_{max}[(\tilde{P}_{T}^{20,3})^{-1}]\sigma_{max}[E_{C}^{24,3}]$$
$$= 1.8 \times 0.15 = 0.27.$$

The magnitude of multiplicative error $|l_d(s)|$ representing scalar dynamic uncertainties in (14) (by $p(s) = \tilde{p}(s)[1 + l_d(s)]$) is given by a formula in Laughlin *et al.* (1987). Magnitude of the resulting $l_m(s)$ in (19) is displayed in Fig. 8. The IMC filter parameter required to detune the controller in (18) for robust performance with respect to perturbation $L_m(s)$ and the performance weight $w(s)$ defined by (2) with $b = 1/2$ and $a = 4$ is $\epsilon = 2.6$. When the indicated nominal

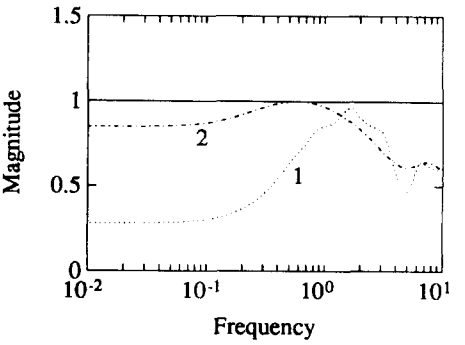

FIG. 7. Plots of $\mu(\omega)$ for the CD response control systems designed in Section 6.2. Curve 1 is $\mu(\omega)$ for the SISO system [this is a conservative bound on $\mu(\omega)$ for the MIMO system with no interaction uncertainties]. Curve 2 is $\mu(\omega)$ for the MIMO system with interaction and actuator uncertainties covered with a conservative norm-bounded multiplicative complex uncertainty.

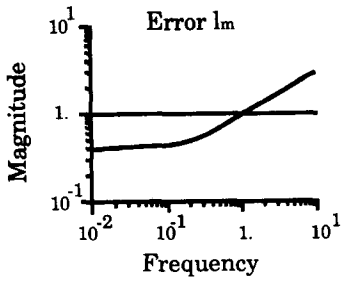

FIG. 8. Magnitude of multiplicative error $l_m(s)$ used for the model-inverse-based design in Section 6.2 with interaction parameter uncertainties.

model and single multiplicative perturbation $L_m(s)$ are considered in this example $\mu(\omega)$ is easily calculated because the nominal loop transfer function is scalar $p(s)c(s)$ times identity. The plot of $\mu(\omega)$ for this design is displayed as Curve 2 in Fig. 7. Robustness with respect to interaction parameter uncertainties requires greater detuning of the controller—bandwidth of the nominal control system is reduced to achieve robustness with respect to perturbation $L_m(s)$. Conservativeness introduced by using the lumped uncertainty $L_m(s)$ in the design procedure will be more severe for high condition number processes.

6.3. *Generality of proposed design methods*

Consider CD response interactions in Table 1 to be elements in $P_T^{20,m}$, where m is the appropriate integer. Eigenvalue bounds for the models calculated from $P_C^{20+2(m-1),m}$ are displayed in Table 2. The ratios $\lambda_{max}/\lambda_{min}$ equal to condition numbers for positive definite models are listed in Table 2 as well. Table 2 indicates that the diagonal controller design procedure developed in this paper can be applied to eight of the models reported in the literature (those that are positive definite). The model-inverse-based or banded (from Laughlin, 1988) controller design procedure would have to be used for models that are not positive definite.

TABLE 2. CONDITION NUMBERS AND EIGENVALUE BOUNDS FOR CD RESPONSE MODELS IN TABLE 1

	λ_{min}	λ_{max}	γ
(1)*	−1.2	2.44	
(2)	−0.9	1.16	
(3)	0.20	1.80	9.00
(4)	0.74	1.38	1.86
(5)	0.60	1.40	2.33
(6)	0.20	1.80	9.00
(7)	−1.0	1.25	
(8)*	0.20	1.01	5.05
(9)*	0.19	3.26	17.2
(10)*	−0.4	6.40	
(11)*	−1.0	1.18	
(12)*	0.20	1.19	5.95
(13)*	0.60	1.13	1.88

See legend to Table 1.

7. CONCLUSIONS

The procedure presented in this paper enables design of robust, large-dimension, diagonal controllers for CD response in paper manufacturing. Robust performance is addressed in the spirit of the structured singular value theory by Doyle (1982). Robust performance of a particular SISO control system design based on singular value bounds of the CD interaction matrix *implies* robust performance of the corresponding MIMO system despite interaction parameter uncertanties. Moreover, the control system based on such a design exhibits robust actuator/sensor failure tolerance.

The robust controller design procedure developed in this paper is applicable to cross-machine-direction control problems other than paper basis-weight control. Similar interaction models result, regardless of the CD response being controlled or the actuator selected. Other candidate CD control systems in the paper manufacturing industry include: water sprays immediately downstream of the slice for CD basis-weight control (Wallace, 1981); hot and cold air showers on calendar stack for CD caliper control (Wilhelm and Fjeld, 1983); sectionalized steam boxes or steam showers for CD moisture control (Wallace, 1981). Applications outside the paper manufacturing industry include plastic sheet fabrication and thin film coating operations (Braatz *et al.*, 1992). Whenever wide flat sheets of uniform products are manufactured, a similar control problem is encountered.

It was shown that the paper machine slice actuator has a significant effect on interactions in the CD response model. The CD basis-weight response model can be tailored to improve controllability with the aid of the dimensionless slice design parameter D_a and slice actuator model. Cross-machine-direction response models can be calculated as direct functions of D_a if basis-weight is assumed to be proportional to the area under the slice in Fig. 3 (this assumption corresponds to an infinitely fast machine with no CD wave propagation on the Fourdrinier wire). Eigenvalues and condition number bounds based on $P_C^{20+2(m-1),m}$ for the resulting CD response models $P_T^{20,m}$ are plotted as functions of D_a in Fig. 9. Recall that in the proposed controller design procedures large condition numbers translate into large gain uncertainty—hence the sufficient conditions for robust performance require highly detuned controllers. Robust

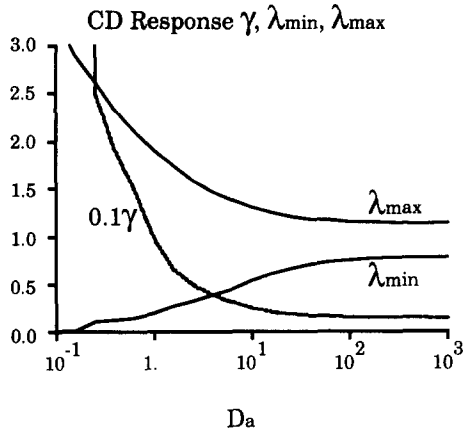

FIG. 9. Eigenvalue and condition number bounds of CD response model $P_T^{20,m}$ as functions of the dimensionless actuator design parameter D_a (assuming no CD wave propagation on the Fourdrinier wire).

diagonal controllers with good performance are therefore possible on paper machines with slices described by large values of D_A. Since elimination of narrow, uneven streaks in paper requires narrow actuator spacing, more flexible slices are necessary to maintain large D_A if a diagonal or banded controller is desired. In his review of the application of control methods to the pulp and paper industry, Dumont (1986) recognizes that, because the industry is old, many mills were not designed with concern for their controllability. Upgrading slice actuators with CD control in mind may well be required.

Acknowledgement—Partial support from the National Science Foundation is gratefully acknowledged.

REFERENCES

Aitken, A. C. (1954). *Determinants and Matrices*, pp. 121–125. Interscience Publishers, New York.

Balas, G. J., A. K. Packard, J. C. Doyle, K. Glover and R. S. R. Smith (1991). Development of advanced control design software for researchers and engineers. *Proc. of the 1991 American Control Conf.*, pp. 996–1001, Boston, MA.

Beecher, A. E., and R. A. Bareiss (1970). Theory and practice of automatic control of basis weight profiles. *Tappi*, **53**, 847–852.

Bellman, R. (1970). *Introduction to Matrix Analysis*, pp. 231–248. McGraw Hill, New York.

Bergh, L. G., and J. F. MacGregor (1987). Spatial control of sheet and film forming processes. *Canadian J. of Chemical Engineering*, **65**, 148–155.

Boyle, T. J. (1978). Practical algorithms for cross-direction control. *Tappi*, **61**, 77–80.

Braatz, R. D., M. L. Tyler, M. Morari, F. R. Pranckh and L. Sartor (1992). Identification and cross-directional control of coating processes. *AIChE J.*, **38**, 1329–1340.

Carey, E. W., C. R. Bietry and H. W. Stoll (1975). Performance factors associated with profile control of basis weight on a paper machine. *Tappi*, **58**, 75–78.

Cuffey, W. H. (1957). Some factors involved in basis weight uniformity. *Tappi*, **40**, 190A–197A.

Davis, P. J. (1979). *Circulant Matrices*, John Wiley and Sons, New York.

Doyle, J. C. (1982). Analysis of feedback systems with structured uncertainties. *IEE Proc. Pt. D*, **129**, 242–250.

Doyle, J. C. (1987). A review of μ for case studies in robust control. *IFAC World Congress*, Munich.

Dumont, G. A. (1986). Application of advanced control methods in the pulp and paper industry—a survey. *Automatica*, **22**, 143–153.

Karlsson, H., I. Lundqvist and T. Ostman (1982). Principles and potentials of CD-basis weight control. *Proc. of the EUCEPA Symp. on Control Systems in the Pulp and Paper Industry*, Stockholm, Sweden, pp. 238–243.

Karlsson, H., and L. Haglund (1983). Optimal cross-direction basis weight and moisture profile control on paper machines. *Proc. of the 3rd Int. Pulp and Paper Process Control Symp.*, Vancouver, Canada, pp. 139–145.

Laughlin, D. L., K. G. Jordan and M. Morari (1986). Internal model control and process uncertainty: mapping uncertainty regions for SISO controller design. *Int. J. Control*, **44**, 1675–1698.

Laughlin, D. L., D. E. Rivera and M. Morari (1987). Smith predictor design for robust performance. *Int. J. Control*, **46**, 477–504.

Laughlin, D. L. (1988). Control system design for robust performance despite model parameter uncertainties: application to cross-directional response control in paper manufacturing. Ph.D. thesis, California Institute of Technology.

McFarlin, D. A. (1983). Control of cross-machine sheet properties on paper machines. *Proc. of the 3rd Int. Pulp and Paper Process Control Symp.*, Vancouver, Canada, pp. 49–54.

Martino, R. (1991). Motor-driven cams actuator flexible-lip automatic die. *Modern Plastics*, **68**, 23.

Morari, M. (1985). Robust stability of systems with integral control. *IEEE Trans. Aut. Control*, **AC-30**, 574–577.

Morari, M. and E. Zafiriou (1989). *Robust Process Control*. Prentice-Hall, Englewood Cliffs, NJ.

Packard, A. K. (1988). What's new with μ: structured uncertainty in multivariable control. Ph.D. thesis, University of California, Berkeley.

Richards, G. A. (1982). Cross direction weight control. *Japan Pulp and Paper*, pp. 41–53.

Skogestad, S., M. Morari and J. C. Doyle (1988). Robust control of ill-conditioned plants: high purity distillation. *IEEE Trans. Aut. Control*, **33**, 1092–1105.

Skogestad, S., and M. Morari (1989). Robust performance of decentralized control systems by independent designs. *Automatica*, **25**, 119–125.

Tong, R. M. (1976). Automatic control of grammage profile on a paper machine. *Proc. of the 3rd IFAC PRP Conference*, Brussels, Belgium, pp. 289–298.

Wallace, B. W. (1981). Economic benefits offered by computerized profile control of weight, moisture, and caliper. *Tappi*, **64**, 79–83.

White, F. M. (1979). *Fluid Mechanics*, pp. 579–601. McGraw-Hill, New York.

Wilhelm, R. G., and M. Fjeld (1983). Control algorithms for cross directional control. *5th Int. IFAC/IMEKO Conf. on Instrum. and Autom. in the Paper, Rubber, Plastics and Polymerization Industries*, Antwerp, Belgium, pp. 163–174.

Wilkinson, A. J., and A. Hering (1983). A new control technique for cross machine control of basis weight. *Preprints of the 5th IFAC PRP Conference*, Antwerp, Belgium, pp. 151–155.

Wrist, P. E. (1961). Dynamics of sheet formation on the Fourdrinier machine. *Oxford Symposium on Formation and Structure*, pp. 839–899.

APPENDIX: PROOFS

This appendix contains proofs for the theorems presented in the paper. First bounds on singular values (and hence bounds on eigenvalues for positive definite $P_{CD}^{n,m}$) of CD response interaction models $P_{CD}^{n,m}$ are derived. All eigenvalues of $P_T^{n,m}$ and appropriately scaled $P_{CSS}^{n,m}$ are found on the same segment of the real axis as are those of a corresponding matrix $P_C^{n+2(m-1),m}$. The bounds form the basis for the robust stability, robust performance and robust failure tolerance results in Theorems 1–3 in which this segment of the real axis is treated as if it were gain uncertainty in a SISO model.

Bounds from singular values of $P_C^{n+2(m-1),m}$

Lemma 5 establishes that the singular values of positive definite symmetric $P_T^{n,m}$ and $P_{CSS}^{n,m}$ are bounded by those of positive definite symmetric $P_C^{n+2(m-1),m}$. Lemma 4 is used to prove Lemma 5. Theorems 1–3 follow from Lemma 5.

Lemma 4. The singular values of matrix A bound the singular values of matrix B when $A \in \mathcal{R}^{q\times q}$ is a real symmetric matrix and $B \in \mathcal{R}^{n\times n}$ $(n<q)$ is equal to R^TAR where $R \in \mathcal{R}^{q\times n}$ is such that $R^TR = I^{n\times n}$:

$$\sigma_{\min}(A) \le \sigma_{\min}(B) \le \sigma_{\max}(B) \le \sigma_{\max}(A).$$

Proof of Lemma 4. Since matrix A is symmetric, $A = A^{1/2}A^{1/2}$, where $A^{1/2}$ is symmetric. Since $R^T \in \mathcal{R}^{n\times q}$ the range of R is a subset of $\mathcal{R}^q$. Then, by definition

$$\sigma_{\max}(A^{1/2}) = \max_{\vec{x}\in\mathcal{R}^q\neq 0} \frac{\|A^{1/2}\vec{x}\|_2}{\|\vec{x}\|_2} \ge \max_{\vec{x}\in \text{Range}\,(R)\neq 0} \frac{\|A^{1/2}\vec{x}\|_2}{\|\vec{x}\|_2}$$

because the maximization on the right occurs over a smaller set $\vec{x} \in \text{Range}\,(R) \subset \mathcal{R}^q$. Since $R\vec{y}$ is nontrivial for all nontrivial $\vec{y}$:

$$\max_{\vec{x}\in\text{Range}\,(R)\neq 0} \frac{\|A^{1/2}\vec{x}\|_2}{\|\vec{x}\|_2} = \max_{\vec{y}\in\mathcal{R}^n\neq 0} \frac{\|A^{1/2}R\vec{y}\|_2}{\|R\vec{y}\|_2}.$$

When A is symmetric, then $B = R^TAR$ is symmetric and the following equalities hold:

$$\begin{aligned}\max_{\vec{y}\neq 0}\frac{\|A^{1/2}R\vec{y}\|_2}{\|R\vec{y}\|_2} &= \max_{\vec{y}\neq 0}\left[\frac{\vec{y}^TR^T(A^{1/2})^TA^{1/2}R\vec{y}}{\vec{y}^TR^TR\vec{y}}\right]^{1/2}\\ &= \max_{\vec{y}\neq 0}\left[\frac{\vec{y}^TR^TAR\vec{y}}{\vec{y}^T\vec{y}}\right]^{1/2}\\ &= \max_{\vec{y}\neq 0}\left[\frac{\vec{y}^TB\vec{y}}{\vec{y}^T\vec{y}}\right]^{1/2}\\ &= \max_{\vec{y}\neq 0}\left[\frac{\vec{y}^T(B^{1/2})^TB^{1/2}\vec{y}}{\vec{y}^T\vec{y}}\right]^{1/2}\\ &= \max_{\vec{y}\neq 0}\frac{\|B^{1/2}\vec{y}\|_2}{\|\vec{y}\|_2}\\ &= \sigma_{\max}(B^{1/2}).\end{aligned}$$

Therefore, $\sigma_{\max}(A^{1/2}) \ge \sigma_{\max}(B^{1/2})$ and $\sigma_{\max}(A) \ge \sigma_{\max}(B)$ when A is symmetric. The same analysis with max replaced by min and $\ge$ replaced by $\le$ leads to $\sigma_{\min}(A^{1/2}) \le \sigma_{\min}(B^{1/2})$ and $\sigma_{\min}(A) \le \sigma_{\min}(B)$ when A is symmetric.

Further, if A is positive definite, then

$$\langle R\vec{y}, AR\vec{y}\rangle = \langle \vec{y}, R^TAR\vec{y}\rangle = \langle \vec{y}, B\vec{y}\rangle > 0 \quad \forall \vec{y} \neq 0$$

so B is positive definite. □

Since matrices $P_T^{n,m}$ and $P_{CSS}^{n,m}$ result from transformations

$$(S^{n,m})^{1/2}R^TAR(S^{n,m})^{1/2}$$

where matrix A is $P_C^{n+2(m-1),m}$, Lemma 4 can be used to bound their singular values by those of the circulant symmetric matrix.

Lemma 5. If $P_C^{q+2(m-1),m}$ is positive definite symmetric, then $P_T^{n,m}$ and $P_{CSS}^{n,m}$ defined by Transformations 1 and 2 are positive definite symmetric and singular values of $P_C^{q+2(m-1),m}$ bound the singular values of matrices $P_T^{n,m}$ and $P_{CSS}^{n,m}$ as follows for all dimensions $n \le q$:

$$\sigma_{\min}(P_C^{q+2(m-1),m}) \le \sigma_i(P_T^{n,m}) \le \sigma_{\max}(P_C^{q+2(m-1),m})$$

$$\sigma_{\min}(P_C^{q+2(m-1),m}) \le \sigma_i((S_{CSS}^{n,m})^{-1/2}P_{CSS}^{n,m}(S_{CSS}^{n,m})^{-1/2}) \le \sigma_{\max}(P_C^{q+2(m-1),m}).$$

Proof of Lemma 5. Matrix $P_C^{q+2(m-1),m}$ from which matrices $P_T^{n,m}$ and $P_{CSS}^{n,m}$ are derived in Transformation 1 and 2 is symmetric. Let $P_C^{q+2(m-1),m}$ be positive definite as well. By definition, $R^TR = I^{n\times n}$ in Transformation 1. Also by definition matrix $S_{CSS}^{n,m}$ in Transformation 2 is real positive definite diagonal. Therefore Lemma 4 proves the bounds on singular values of $P_T^{n,m}$ and $P_{CSS}^{n,m}$ and that $P_T^{n,m}$ and $P_{CSS}^{n,m}$ are positive definite for all dimensions $n \le q$. □

Lemma 4 exploits the knowledge that Toeplitz symmetric matrices are cut out of the center of a larger dimension circulant symmetric matrix through Transformation 1. Lemma 5 then guarantees that eigenvalues of positive definite $P_C^{q+2(m-1),m}$ will bound those of $P_T^{n,m}$ for all dimensions n less than or equal to q. Since centrosymmetric matrices $P_{CSS}^{n,m}$ are derived from Toeplitz symmetric matrices through Transformation 2, their eigenvalues can be bounded by those of a higher dimension circulant symmetric matrix as well.

Proofs of Theorems 1–3

Proof of Theorem 1. If $P_C^{q+2(m-1),m}$ is positive definite symmetric, then by Lemma 5 the following matrices with $n \le q$ are positive definite symmetric with eigenvalues $\lambda_i \in [\sigma_{\min}(P_C^{q+2(m-1),m}), \sigma_{\max}(P_C^{q+2(m-1),m})]$:

$$P_C^{n+2(m-1),m}$$

$$P_T^{n,m}$$

$$(S_{CSS}^{n,m})^{-1/2}P_{CSS}^{n,m}(S_{CSS}^{n,m})^{1/2}.$$

Each of the symmetric matrices above can be expressed as $U\Lambda U^T$, where U is unitary, and $\Lambda = \text{diag}\,(\lambda_i)$. Since the SISO control system with loop transfer function $kp(s)c(s)$ is robustly stable for all $p(s)$ and for all $k \in \lambda_i$, the fully diagonal MIMO control system with loop transfer function $\Lambda p(s)c(s)$ is robustly stable for all dimensions $n \le q$. (Robust stability for a fully diagonal system is equivalent to robust stability of all individual loops.) Premultiplication of the loop transfer function by U and postmultiplication by $U^T = U^{-1}$ do not change the robust stability of the system. Therefore the MIMO control system with loop transfer function $U\Lambda p(s)c(s)U^T$ is robustly stable. Since $p(s)$ and $c(s)$ are scalars, the control system with loop transfer function $U\Lambda U^Tp(s)c(s)$ is robustly stable. Now $U\Lambda U^T$ is equal to $(S_{CSS}^{n,m})^{-1/2}P_{CSS}^{n,m}(S_{CSS}^{n,m})^{-1/2}$ for the third matrix above where $S_{CSS}^{n,m}$ is either scalar times identity or centrosymmetric diagonal. Premultiplication of $(S_{CSS}^{n,m})^{-1/2}P_{CSS}^{n,m}(S_{CSS}^{n,m})^{-1/2}$ by $(S_{CSS}^{n,m})^{1/2}$ and postmultiplication by $(S_{CSS}^{n,m})^{-1/2}$ and the fact that diagonal matrices commute with one another proves the robust stability results. □

Proof of Theorem 2. If $P_C^{q+2(m-1),m}$ is positive definite symmetric, then by Theorem 1 the three matrices highlighted in the proof of Theorem 1 are positive definite symmetric with eigenvalues $\lambda_i \in [\sigma_{\min}(P_C^{q+2(m-1),m}), \sigma_{\max}(P_C^{q+2(m-1),m})]$. Therefore, each of the matrices can be expressed as $U\Lambda U^T$ where U is unitary, and $\Lambda = \text{diag}\,(\lambda_i)$. Since the SISO control system with loop transfer function

$kp(s)c(s)$ exhibits robust performance in the sense that $|w(i\omega)(1+kp(i\omega)c(i\omega))^{-1}|<1$ for all ω, for all $p(s)\in\pi$, and for all $k=\lambda_i$, the fully diagonal MIMO control system with loop transfer function $\Lambda p(s)c(s)$ exhibits robust performance in the sense that

$$\sigma_{\max}[w(i\omega)(I+\Lambda p(i\omega)c(i\omega))^{-1}]<1 \quad \forall\omega$$

for all $p(s)\in\pi$. (The maximal singular value of a diagonal matrix is equal to the magnitude of the largest diagonal element.) The maximum singular value is invariant to unitary transformation, so

$$\sigma_{\max}[w(i\omega)(I+U\Lambda p(i\omega)c(i\omega)U^T)^{-1}]<1 \quad \forall\omega.$$

Since $p(i\omega)$ and $c(i\omega)$ are scalars,

$$\sigma_{\max}[w(i\omega)(I+U\Lambda U^T p(i\omega)c(i\omega))^{-1}]<1 \quad \forall\omega.$$

Now $U\Lambda U^T$ is equal to $(S_{CSS}^{n,m})^{-1/2}P_{CSS}^{n,m}(S_{CSS}^{n,m})^{-1/2}$ in the third matrix listed in the proof of Theorem 1 above, where $S_{CSS}^{n,m}$ is centrosymmetric diagonal. Premultiplication of

$$[w(i\omega)(I+U\Lambda U^T p(i\omega)c(i\omega))^{-1}]$$

by $(S_{CSS}^{n,m})^{1/2}$ and postmultiplication by $(S_{CSS}^{n,m})^{-1/2}$ do not change its maximum singular value $\sigma_{\max}$ when $S_{CSS}^{n,m}$ is centrosymmetric diagonal. This establishes the robust performance results. □

Proof of Theorem 3. If $P_C^{q+2(m-1),m}$ is positive definite symmetric, then by Lemma 5 the three matrices highlighted in the proof of Theorem 1 are positive definite symmetric with eigenvalues $\lambda_i\in[\sigma_{\min}(P_C^{q+2(m-1),m}),\ \sigma_{\max}(P_C^{q+2(m-1),m}]$. Actuator/sensor failure is equivalent to premultiplication and postmultiplication of these three matrices by R^T and R, respectively, where $R\in\mathcal{R}^{m\times r}$ is a matrix with $r<n$ such that $R^TR=I^{r\times r}$. By Lemma 4 the eigenvalues of

$$R^TXR$$

where X is one of the three matrices listed in the proof of Lemma 5 above, are bounded on the real axis by $\sigma_{\min}(P_C^{q+2(m-1),m})$ and $\sigma_{\max}(P_C^{q+2(m-1),m})$. Therefore, theorems 1 and 2 with the fact that $S^{n\times n}R^{n\times r}=R^{n\times r}S^{r\times r}$ for diagonal matrices S (appropriate rows and columns of $S^{n\times n}$ are eliminated in $S^{r\times r}$) prove the robust stability and robust performance results for actuator/sensor failure. □